Available online at www.sciencedirect.com
ScienceDirect
Journal of the European Ceramic Society 27 (2007) 3149–3159
www.elsevier.com/locate/jeurceramsoc

Nanoscaled $BaTiO_3$ powders with a large surface area synthesized by precipitation from aqueous solutions: Preparation, characterization and sintering

W. Lu [a,*], M. Quilitz [a,b], H. Schmidt [b]

[a] *Leibniz-Institut für Neue Materialien gem. GmbH, Im Stadtwald, Gebäude D2 2, D-66123 Saarbrücken, Germany*
[b] *Lehrstuhl für Neue Materialien, Universität des Saarlandes, Beethovenstrasse Z4, D-66125 Saarbrücken, Germany*

Received 5 July 2006; received in revised form 2 January 2007; accepted 7 January 2007
Available online 15 February 2007

Abstract

Nanosized $BaTiO_3$ powders with a specific surface area of 60–75 m^2/g have been prepared by precipitation of a titanium ester with $Ba(OH)_2$ solution at temperatures less than 100 °C. The effects of the $Ba(OH)_2$ concentration, isopropanol mixing with water as a solvent, the Ba:Ti ratio and surface modifiers on the surface area, the particle size, the crystalline phase, the agglomeration and aggregation degree of the synthesized powders as well as dielectric properties of sintered pellets have been investigated. The properties of the obtained powders have been characterized with XRD, BET, TG-DTA, ICP-AES, HRTEM and dilatometer. A high concentration of $Ba(OH)_2$ can increase the agglomeration and aggregation degree of the particles while the addition of isopropanol in water is beneficial for lowering it. To obtain stoichiometrical barium titanate, the ratio of Ba:Ti should be 1.1. The leaching of barium ions during processing can be limited by washing the powder with ammonia solution at pH10.2. A $BaTiO_3$ ceramic (95.8% of the theoretic density) has been fabricated by sintering the powders at 1250 °C for 2 h.

Keywords: Powders-chemical preparation; Sintering; Thermal properties; $BaTiO_3$; Capacitors

1. Introduction

The extensive application of barium titanate ($BaTiO_3$) in the ceramic industry is based on the properties of its polymorphs.[1,2] At temperatures higher than about 130 °C (Curie temperature), $BaTiO_3$ exists in the cubic perovskite structure. In this crystal structure, the Ba^{2+} ions occupy the corners of the elementary cell, the Ti^{4+} ions the volume centre and the O^{2-} ions the surface centre. Because of the high symmetry of the cubic phase barium titanate exhibits paraelectricity and an isotropic dielectricity. Below the Curie point, the crystal structure transforms from the cubic phase to the distorted tetragonal structure with a displacement of the centres of positive and negative charges within the sublattice. As a result, a dipole moment parallel to one of the cubic axes of the original phase arises. Such generated spontaneous polarization in the tetragonal structure is the origin of its ferroelectric and piezoelectric behaviour. Further reduction of the temperature changes the structure of barium titanate into an orthorhombic structure at about 5 °C and finally into the rhombohedral structure at 90 °C. In fact, little study has been done for the latter two low-temperature modifications of $BaTiO_3$ and also no industrial application of them has been reported. Cubic and tetragonal $BaTiO_3$ phases exhibit high dielectric constants. The dielectric constant of barium titanate ceramic prepared from fine powders varies from 1500 to 6000 at room temperature.[3] As a dielectric material, $BaTiO_3$ is mainly used for capacitors such as multilayer ceramic capacitors (MLCCs)[4] and integral capacitors in printed circuit boards (PCB).[5] Its polarization below Curie point can be applied for the use in dynamic random access memories (DRAM).[6] Its piezoelectric properties enable its use in transducers and actuators.[7] $BaTiO_3$ is also a semiconducting and a non-linear optic material when doped with other elements, and therefore can be used for resistors with positive temperature coefficient of resistivity (PTCR),[8] temperature–humidity-gas sensors[9] as well as electro-optic devices.[10]

The recent advances in electronic devices prepared from barium titanate show the trend of continuous miniaturization and improved performance. For MLCCs, this means higher capacitance in smaller case sizes. The strategies taken for this are to

* Corresponding author. Tel.: +49 681 9300337; fax: +49 681 9300223.

0955-2219/$ – see front matter © 2007 Elsevier Ltd. All rights reserved.
doi:10.1016/j.jeurceramsoc.2007.01.002

increase the number of active layers to 200–400 and to lower the dielectric layer thickness below 2–3 μm.[11] Important properties of capacitors such as break down voltage and DC leakage are dependent on the layer thickness, grain size and pore defects. The effective dielectric layer is believed to be several, e.g. at least 3–5, grains thick.[12] To meet the market requirements for miniaturization of MLCCs, therefore $BaTiO_3$ powders with nanometer-sized particles, a large surface area as well as high homogeneity are required to achieve good sinterability and fine grained microstructure in sintered ceramics. For similar reasons, nanosized barium titanates are also thought to be ideal starting powders for PCB, DRAM and other applications.

Conventionally, the $BaTiO_3$ powder was prepared by the solid-state reaction method through heating $BaCO_3$ and TiO_2 at temperatures as high as 1200 °C.[13,14] To obtain fine $BaTiO_3$ powders with high quality, many new synthesizing methods have been developed, including sol–gel method,[15–17] Pechini processing[18–20] using a citric or oxalate complex as the precursor, hydrothermal synthesis[21–23] and precipitation method from aqueous solution. In the sol–gel process, $BaTiO_3$ gels can be obtained by hydrolysing the metal alkoxide. The most advantageous characteristics of this method are the high purity and the excellent control of the composition of the resulting powders. To crystallize $BaTiO_3$, however, the hydrolysis product should normally be calcined at temperatures above 500 °C. The expensive raw materials and the low yield rate are the main hindrances for the commercial application of this method. The advantage of the Pechini process lies in the limitation of segregation of various metal ions, and is achieved by forming stable metal-chelate complexes with a stoichiometric Ba:Ti ratio of 1:1. The pyrolysis of the complexes often occurs at a temperature ranging from 500 to 1000 °C, which unavoidably results in aggregation of $BaTiO_3$ particles. In contrast to this, hydrothermal synthesis can lower the processing temperature to 100–250 °C. The prepared $BaTiO_3$ powders with relative uniform particles also showing narrow size distributions. However, the average particle size of most powders is larger than 100 nm. Using this method, it is very difficult to prepare $BaTiO_3$ with a specific surface area larger than 30 m^2/g (corresponding to an average particle size of about 33 nm).

Preparation of $BaTiO_3$ powders directly from aqueous solution by precipitation facilitates the process-control and the property tailoring of the end-powder. Furthermore, it will make the continuous large-scale production easier, compared to other synthesis routes. The precipitation of $BaTiO_3$ upon addition of a titanium ester to an aqueous solution of a soluble barium salt above 80 °C was first reported by Flaschen.[24] Using solvent media of controlled polarity, Kiss et al.[25] synthesized high-purity $BaTiO_3$ from the triethanolamine chelate of tetraisopropyl titanate at 80–90 °C. Recently, routes for synthesizing nanosized $BaTiO_3$ from titanium alkoxide modified with, e.g. glacial acetic acid[26] or acetylacetone[27] in alkaline solution have been developed. Surfactants such as LAS[28] and microbial-derived surfactants[29] were reported to be effective to limit the particle growth by precipitation of $BaTiO_3$ from titanium isopropoxide in aqueous solution. The resulted powders show a small particle size (30–90 nm) and a larger surface area (60.5 m^2/g). A lot of study on using cheap $TiCl_4$ instead of titanium alkoxide for synthesizing $BaTiO_3$ through coprecipitation method at temperatures of 80–100 °C has been done by groups of Nanni et al.,[30–34] Lee and co-workers[35,36] and Matijevic and co-workers[37]. However, a Ba/Ti ratio higher than 1 and excess alkaline solution for keeping pH > 14 should be satisfied for preparing particles in nanosize (30–40 nm). As a result, the removing of ions like Na^+ and Cl^- from the powder by washing will become more difficult. The obtained surface area of powders is also less than 40 m^2/g.[30,32]

Accompanying the decrease of particle size in nanometer through lowering the processing temperature, the size effect of $BaTiO_3$[20,22,38–47] has attracted much attention. It was first observed that the dependence of the permittivity of $BaTiO_3$ on particle size in nanometer range is different from that in micrometer range. Later the cubic $BaTiO_3$ phase is found to be the stable phase in the powder at room-temperature when the particle size is small enough. It is now generally agreed that the transition temperature from cubic (paraelectric) phase to tetragonal (ferroelectric) phase, namely the Curie temperature is size-dependant and it will be lowered with decreasing the particle or the grain size. However, the explanations about the size effect are far from indisputable. The influence of OH^- groups on the lattice is already realized, which is related to the low-temperature synthesis routes.[20,22,40] The critical particle size, at which the cubic-tetragonal transition occurs, on one hand, is very difficult to determine because of the small difference of the lattice constants of both structures. On the other hand, its reported value varies from case to case between 10 and 190 nm[20,22,39–43,47] depending on the synthesis methods and it still lacks an accepted critical particle size value below which the cubic polymorph of $BaTiO_3$ is stabilized. Thus, much work has still to be done to clarify the origin of this effect and to determine the decisive factors, which influence the microstructure of $BaTiO_3$.

In this paper, the precipitation process is chosen to synthesize nanosized $BaTiO_3$ powders. For optimizing the processing various parameters such as the concentration of $Ba(OH)_2$ and the ratio of Ba:Ti have been investigated. We have also studied the influence of the leaching of barium ions during processing on the thermal behavior of the prepared powders. Finally, the $BaTiO_3$ pellets have been sintered and their dielectric properties have been determined.

2. Experimental procedure

A 12.88 g $Ba(OH)_2 \cdot 8H_2O$ was dissolved in the mixture of isopropanol and water by keeping the temperature of the oil bath at 120 °C. Tyzor TE (titanium bis(triethanolamine)diisopropoxide, Dupont) with a given amount was slowly added to this solution under stirring. After its addition, the reaction was kept under refluxing condition for 15 min to 6 h. N_2 was used as a protecting gas to avoid the absorbance of carbon dioxide from the air atmosphere. The precipitate, after separated with a centrifuge at 4000 rpm for 60 min, was washed with distilled water and dried at 60 °C in a vacuum furnace. For surface modification, the surfactant with a concentration of 5 wt.% relative to $BaTiO_3$ was mixed with the $Ba(OH)_2$ solution.

In the experiment, the pH value was measured by a pH meter (pH 535, WTW) with an integrated temperature sensor. The crystalline phase of the powder was analyzed with a D500 model diffractometer (Siemens, radiation Cu $K\alpha_1$) operating at 40 kV. The crystallite size was calculated from Scherrer equation.[48] The thermal behaviour of the samples was analyzed by thermogravimetric analysis and differential thermal analysis (TG-DTA: STA501, Baer). The structure and morphology of powders were studied with a high resolution transmission electron microscope (HRTEM: CM200 FEG, Philips). The specific surface areas of the powders were characterized with a BET gas adsorption analyser (ASAP 2400, Micrometrics). The particle size distribution of the powder was determined using the method of dynamic light scattering (Mastersize 2000, Malvern). The linear shrinkage of pellet samples, which were cold isostatically pressed to a dimension of ca. Ø 5 mm × 5 mm under a pressure of 400 MPa was measured with a differential dilatometer (Linseis). The pellet was heated to 1350 °C at a rate of 5 °C/min in air atmosphere. Samples for sintering were pellets with a dimension of about Ø 10 mm × 1 mm, which were formed under a cold isostatic pressure of 400 MPa. The green body was heated to 1100–1300 °C at 10 °C/min and soaked for 0.5–4 h. The bulk density of the sintering ceramic was measured by the Archimedes method with water as the immersing medium. The surface of the polished sintered samples was investigated with the scanning electron microscope (JSM 6400F, JEOL) using 10 kV accelerating voltage. For the chemical analysis, the mixture of about 50 mg powder samples, 4 g lithium tetraborate and 2 g lithium metaborate were melted at 1000 °C for 1 h. One hundred milligrams of the solidified melt were dissolved in 3 ml concentrated HNO_3 acid at 100 °C. The obtained solution was diluted with distilled water and analyzed using atomic emission spectroscopy with inductively coupled plasma (ICP-AES) for determination of barium and titanium. Dielectric constants and losses were determined with a precision LCR meter (4284 A, Agilent Technologies) at frequencies between 20 and 10^6 Hz. With the experimental set-up capacitances were measured and dielectric constants were calculated from the capacitance data via the equation $C = (\varepsilon_0 \varepsilon_r A)/t$ with C the capacitance, ε_0 the dielectric constant of the free space (8.854×10^{-12} F/m), A the area of the dielectric, t the thickness and ε_r is the dielectric constant of the sample. Dielectric losses could be measured directly using the LCR meter.

3. Results

3.1. Effects of the refluxing time

A 1.5 M $Ba(OH)_2$ water/isopropanol (volume 50:50) solution reacted with stoichiometrical Tyzor TE under refluxing conditions. The precipitate samples at different refluxing time were characterized with the X-ray diffractometer to analyze their phase composition. The XRD patterns in Fig. 1a show that $BaTiO_3$ is well-crystallized in the sample under refluxing conditions within 0.25 h. $BaCO_3$ as a second phase can also be discerned. No obvious change can be observed through extending the refluxing time from 0.25 to 6 h. As the whole reaction was carried out using N_2 gas as the protecting gas, the formation

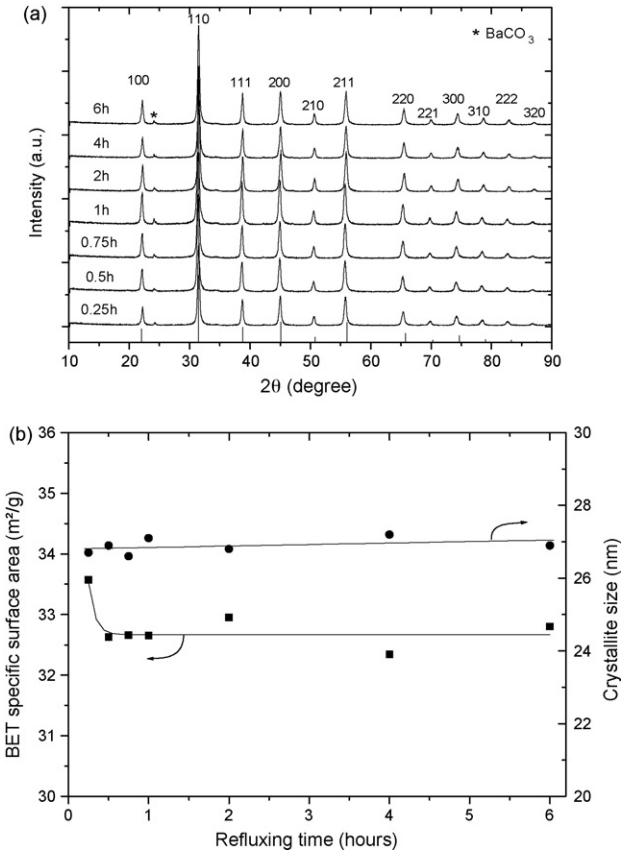

Fig. 1. (a) XRD patterns (the inserted lines correspond to the JCPDS data of 75–212) and (b) BET specific surface area and crystallite size of $BaTiO_3$ powders synthesized by refluxing for 0.25–6 h: 0.15 M $Ba(OH)_2$, volume ratio of isopropanol/aqueous solution = 0.5.

of the impurity of $BaCO_3$ indicates the necessity of degassing the starting solutions for minimizing the amount of $BaCO_3$. The crystallite size of $BaTiO_3$ was calculated from (1 1 0) peak of the corresponding XRD pattern using Scherrer equation. The results are given in Fig. 1b. Although, the change of the crystallite size with extending the refluxing time is small, an increasing trend can still be found. This means, the $BaTiO_3$ crystallite grows with increasing refluxing time. The BET specific surface area of the $BaTiO_3$ powder decreases first and becomes then constant with an increase in refluxing time. It is reported[25] that the extension of the reaction time to 1 h is beneficial to obtain products containing less free titanium dioxide. Here, the results show that a longer reaction time has no positive influence on the crystallization, the crystallite size and the surface area. One hour is therefore determined as the refluxing time for further experiments.

3.2. Effects of the concentration of the $Ba(OH)_2$ solution

$Ba(OH)_2$ as the starting material also influences the pH value of the solution. Controlling its concentration is therefore important for precipitation of the $BaTiO_3$ which depends on the pH value.[49] The concentration referred here is the concentration of $Ba(OH)_2$ in water, although an equal volume of isopropanol is also used as the solvent. $BaTiO_3$ powders were processed at

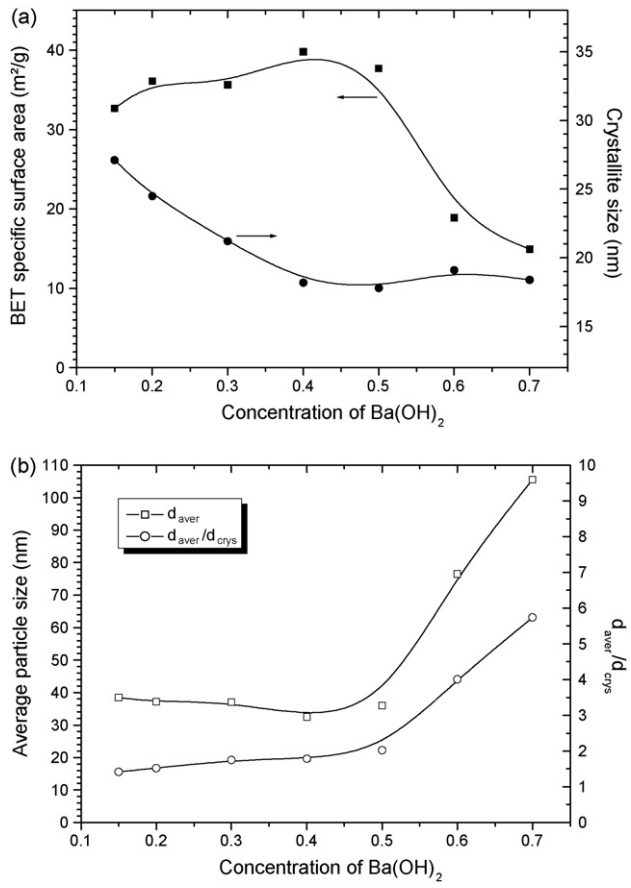

Fig. 2. Dependence of (a) BET specific surface and crystallite size (d_{crys}) and (b) average particle size (d_{aver}) and d_{aver}/d_{crys} on the concentration of $Ba(OH)_2$ aqueous solution. Refluxing time: 1 h, volume ratio of isopropanol/aqueous solution = 0.5.

refluxing conditions for 1 h in solutions that contained varying $Ba(OH)_2$ concentration from 0.15 to 0.7 M.

In the examined concentration range, the prepared powders consist of $BaTiO_3$ and a small amount of $BaCO_3$. The crystallite size (d_{crys}) of $BaTiO_3$ is decreased from 24.5 to 18.2 nm as the concentration of the $Ba(OH)_2$ is increased up to 0.4 M. It changes little with a further increase in concentration of $Ba(OH)_2$ (Fig. 2a). On the other hand, the BET specific surface area of the powder increases gradually to 38.8 m^2/g with increasing the $Ba(OH)_2$ concentration to 0.4 M and then decreases rapidly at higher concentrations.

The average particle size of the powder (d_{aver}, nm) is calculated according to the formula:

$$d_{aver} = \frac{6000}{\rho \times S} \quad (1)$$

where ρ is the measured density of the powder (g/cm^3) and S is the BET specific surface area (m^2/g). The difference between d_{aver} and d_{crys} qualitatively reflects the agglomeration and aggregation degree of the powder. In this work, d_{aver}/d_{crys} is calculated and used as an agglomeration and aggregation index. The larger the value of the index, the more severe the agglomeration and aggregation of particles is. From Fig. 2b, we can see that the average particle size reaches the minimal value of 32.5 nm as the concentration is increased from 0.15 to 0.4 M. From 0.5 M, it increases linearly with the concentration and becomes larger than 100 nm at 0.7 M. Compared to this, the d_{aver}/d_{crys} ratio always increases with an increase in concentration. It increases first slowly in the range of 0.14–0.4 M and then rapidly between 0.5 and 0.7 M. It can be drawn that the agglomeration and aggregation of the $BaTiO_3$ particles at higher concentrations is more severe than at low concentrations.

It was reported by Testino et al.[33] that the mean crystallite size and the mean particle size of $BaTiO_3$ also decreases with increasing concentration of $BaCl_2$ and $TiCl_4$ solutions in the range of 0.035–0.070 M. A secondary nucleation of $BaTiO_3$ on the surface of TiO_2 as the formation mechanism was proposed.[34] To avoid this possible secondary nucleation, the Tyzor TE was added in the $Ba(OH)_2$ solution at the refluxing condition. According to the literature,[39] $BaTiO_3$ can exist in the solution, provided that pH is appropriately chosen. Because of the most possible coprecipitation of the $BaTiO_3$ in our case the nucleation of $BaTiO_3$ from the solution can be regarded as a homogeneous process. At a low barium hydroxide concentration, less nuclei can be formed in the solution, and they can easily grow to be large crystallites. As the concentration is increased, the formation of more nuclei in very short time exhausted the solution rapidly with respect to barium titanate. The transport of solute from the bulk solution to the crystal surface will be more difficult and the particle growth is limited. When the concentration is further increased to a definite value, the rate of nucleation will be limited by collision of molecules by diffusion. The concentration of the solute is then somewhat higher, which becomes again favourable to the particle growth. Because of the balance of the nucleation and growth, the crystallite size of $BaTiO_3$ remains almost unchanged between 0.4 and 0.7 M.

The decrease in primary size of the particle and the increase in particle number with increasing concentration at the low concentration range of 0.15–0.4 M lead to a stronger electrostatic attraction between particles at a higher concentration. As a result, the agglomeration and aggregation degree increases with the concentration. It is well-known that there exists an electric double layer which counteracts that attraction around the particle. The thickness of this layer can be greatly decreased by increasing the ion intensity of the solution. After this layer is depleted at a given counter-ion concentration, the agglomeration and aggregation degree increases substantially. That is why the agglomeration and aggregation of $BaTiO_3$ particles increases rapidly at higher concentrations. The combining effect of $Ba(OH)_2$ concentration on the particle size and the aggregation of particles results in an optimal concentration of $Ba(OH)_2$ at 0.4 M for obtaining $BaTiO_3$ powders with a larger surface area.

3.3. Effects of the isopropanol concentration

The effects of the isopropanol concentration in solution were examined by processing powders under refluxing conditions for 1 h in solutions that contained 0.4 M $Ba(OH)_2$. The volume concentration of isopropanol $V_{isop}/(V_{isop} + V_{H_2O})$ was varied from 0 to 0.8. A higher value will lead to the difficulty in dissolution of $Ba(OH)_2$.

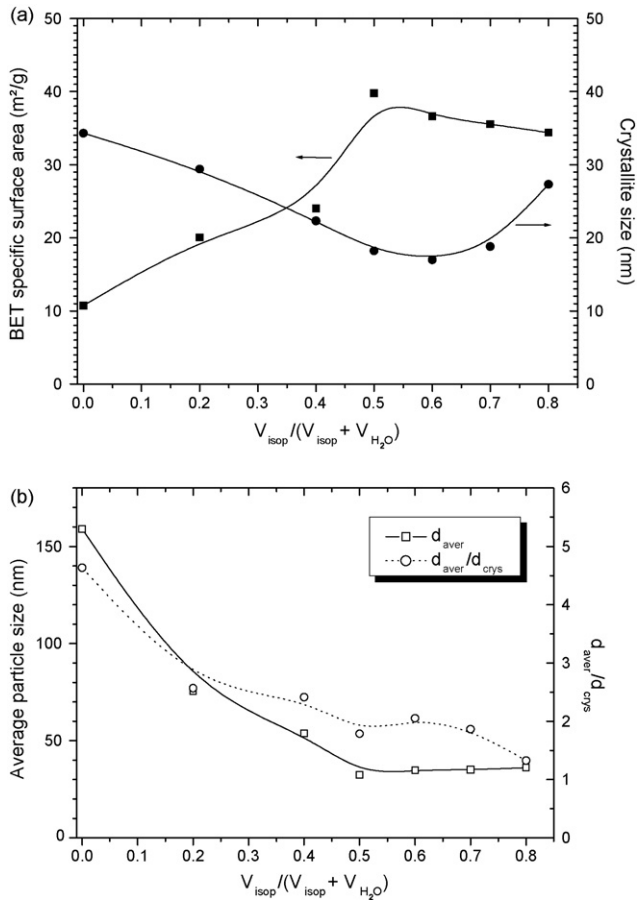

Fig. 3. (a) BET specific surface and crystallite size and (b) average particle size and d_{aver}/d_{crys} of $BaTiO_3$ powders synthesized with different volume ratios of isopropanol to aqueous solution: 0.4 M $Ba(OH)_2$, refluxing time of 1 h.

The import of isopropanol in water does not change the phase composition of the powder, but it influences the crystallite size and the BET specific surface area of $BaTiO_3$ (Fig. 3a). The crystallite size decreases while the specific surface area of the prepared powder increases through increasing the isopropanol concentration up to 0.5. A higher volume percentage of isopropanol in solution than that of water cannot increase the specific surface area of the powder any more but results in a gradual increase in crystallite size.

The dependence of the average particle size (d_{aver}) and the agglomeration and aggregation index d_{aver}/d_{crys} on the isopropanol concentration is shown in Fig. 3b. The average particle size of the powder decreases rapidly from 159 to 32.5 nm by increasing the isopropanol concentration from 0 to 0.5 and keeps then almost unchanged while the d_{aver}/d_{crys} is lowered from 4.6 to 1.3 in the concentration range of 0–0.8.

As described in above, the addition of isopropanol in water decreasing the polarity of the solution shows its effect in lowering the agglomeration and aggregation degree of particles, decreasing the average particle size and the crystallite size as well as increasing the specific surface area. However, a high isopropanol concentration of more than 0.5 will cause an increase in crystallite size and a decrease in specific surface area.

The decrease in polarity of the medium by increasing the amount of isopropanol can lower the solubility of $BaTiO_3$ because that increasing deviations in polarity between the medium and $BaTiO_3$ will make solubility increasingly difficult.[25] The resulting higher supersaturation of $BaTiO_3$ under refluxing conditions leads to a smaller critical size and a larger nucleation rate which limits the particle growth. The decrease in primary size with increasing isopropanol volume in the solution is therefore understandable. An increase in crystallite size from $V_{isop}/(V_{isop} + V_{H_2O}) = 0.6$ is probably due to the low solubility of $Ba(OH)_2$ in isopropanol. The insolvable part of $Ba(OH)_2$ may decrease the supersaturation of $BaTiO_3$ and contributes to the growth of the $BaTiO_3$ nuclei by direct contact with the particle surface.

With increasing isopropanol concentration, more isopropanol molecules will be adsorbed on the surface of the $BaTiO_3$. The resulted increase in hydrophobicity of the particles can lower the attracting force and contribute to a lower agglomeration and aggregation degree. For this reason, the average particle size does not increase at high isopropanol concentrations although the crystallite size increases. The increased specific surface area at low isopropanol concentrations can be attributed to the decrease in particle size.

3.4. Effects of the molar ratio of Ba:Ti in solution

The powders were processed by varying the initial ratio of barium to titanium in solution from 0.8 to 1.2. The solvents used are isopropanol purged by N_2 and boiled water for minimizing the CO_2 concentration in the solution. The obtained powders were washed with distilled water four to six times until the conductivity of the suspension is less than 100 μS/cm.

The XRD patterns of the powders (Fig. 4a) indicate all powders consist of the cubic $BaTiO_3$ phase, independent of the initial Ba:Ti ratio. No trace of $BaCO_3$ can be found.

The BET specific surface area of the powder decreases while the crystallite size increases linearly with the initial ratio of Ba:Ti in solution (Fig. 4b). The well-washed powder at Ba:Ti = 1.0 has a specific surface area of 55.6 m^2/g, compared with that of the as-prepared powder with a value of 39.8 m^2/g.

The molar ratio of barium to titanium in the powder product that resulted from the initial molar ratio of Ba:Ti in the reaction solution is shown in Fig. 4c. If the powder stoichiometries directly reflected the initial solution composition, the experimental data in Fig. 4c would follow the straight line $y = x$ shown in the figure. However, the overall powder stoichiometry deviated from the initial solution composition. Excess barium hydroxide with an initial Ba:Ti ratio of about 1.1 is necessary to obtain the stoichiometric $BaTiO_3$ powder. On the one hand, barium-deficiency is found in the powder when its initial Ba:Ti ratio is less than 1.1. On the other hand, the excess of barium ions in the powder cannot be completely washed out as the initial ratio is larger than 1.1. The dependence of the agglomeration and aggregation degree on the Ba:Ti ratio in solution is also presented in Fig. 4c. The value of d_{aver}/d_{crys} varies in the range of 1.05–1.35, which shows a relative low aggregation between particles. Although, the high Ba:Ti ratio causes

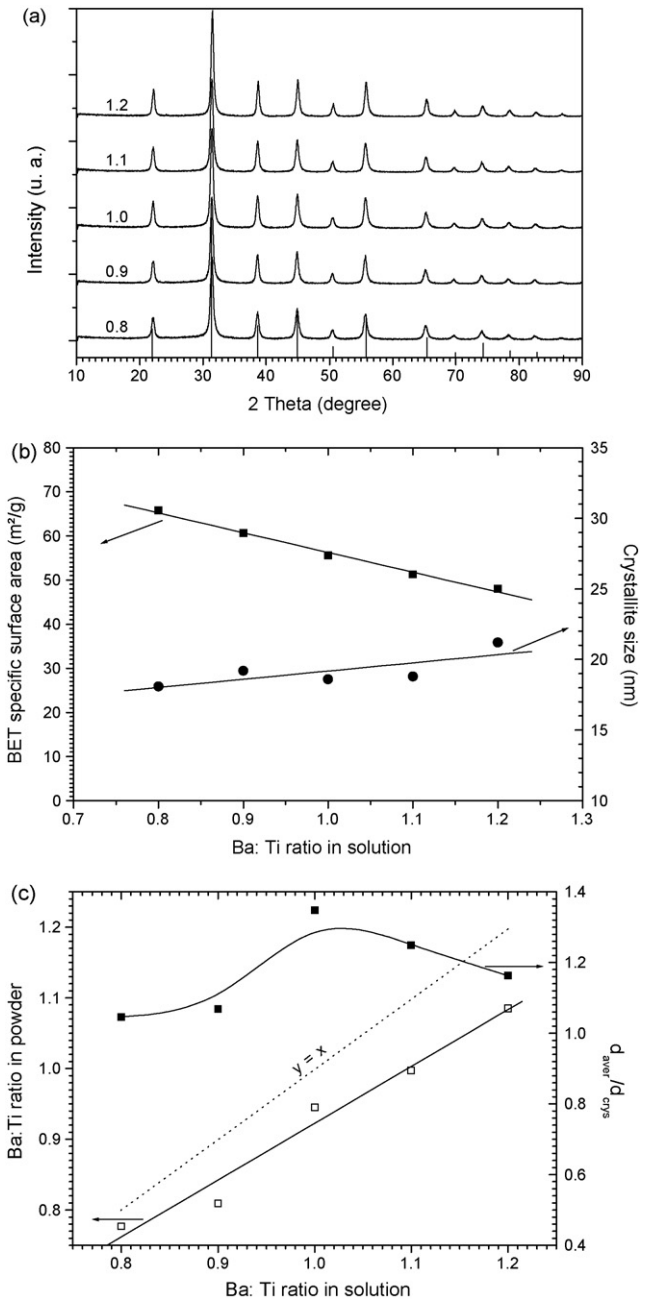

Fig. 4. (a) XRD patterns, (b) BET specific surface and crystallite size and (c) d_{aver}/d_{crys} and Ba:Ti ratio of washed $BaTiO_3$ powders synthesized with different Ba:Ti ratio in solution: 0.4 M $Ba(OH)_2$, refluxing time of 1 h, volume ratio of isopropanol/aqueous solution = 0.5.

the growth of the crystallite (Fig. 4b), it does not result in the particle aggregation.

According to Fig. 4a, it seems that the initial Ba:Ti ratio does not influence the phase composition of the powder even the powder stoichiometries deviate from the initial solution composition. However, the effects of the composition deviation on the powders can be detected after their being calcined at 1000 °C for 2 h. The XRD spectra of the calcined powders are shown in Fig. 5. At Ba:Ti = 0.8, the calcined powder consists of tetragonal $BaTiO_3$ and $BaTi_2O_5$. Obviously, the latter is formed through reacting $BaTiO_3$ with excess titanium in the powder at high tempera-

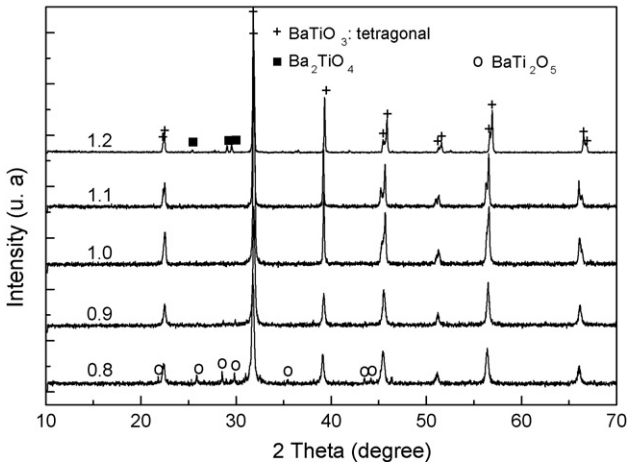

Fig. 5. XRD diagrams of powders calcined at 1000 °C for 2 h, which were synthesized with different Ba:Ti ratio.

tures. At Ba:Ti = 1.2, the barium-rich titanate phase of Ba_2TiO_4 is found in the calcined powder besides tetragonal $BaTiO_3$. From 0.9 to 1.1, the calcined powders consist of the $BaTiO_3$ phase.

The above results clearly show the negative effect on the purity of the powder when excess barium or titanium is used for preparing barium titanate. In the as-prepared powder, the excess titanium at low Ba:Ti ratios exists as amorphous TiO_2 phase while at high Ba:Ti ratios some of the excess barium ions can be adsorbed on the surface of the $BaTiO_3$ particle (part of excess barium is eliminated by washing, see Fig. 4c). The amorphous phase, when its amount in powder is low, cannot be detected by the ordinary XRD. Thus, we cannot observe any change in phase composition of the as-prepared powder with increasing the Ba:Ti ratio. It should be pointed out that the amorphous titanium oxide in the Ti-rich samples, normally with a high specific surface area will contributes to their large specific surface area (Fig. 4b).

The tetragonal $BaTiO_3$ phase in the powder is characterized by the splitting of the peaks of (2 2 0) and (2 0 2) at 45°. The influence of the Ba:Ti ratio on the tetragonality of $BaTiO_3$ can also be reflected from Fig. 5. In the samples with a lower Ba:Ti ratio, the tetragonality is so low that the splitting of these two peaks is still not obvious. The higher tetragonality can nevertheless be easily found from the well-splitted peaks in the Ba-rich powders.

3.5. Effects of the leaching of barium from barium titanate

The leaching of barium from barium titanate in water is found to be dependent on pH and to increase with decreasing pH.[50,51] To investigate the effects of barium dissolution in water the $BaTiO_3$ powders prepared with a initial Ba:Ti ratio of 1.0 were washed with acetic acid to pH 6.5, with deionised water to pH 8.6 and with ammonia solution to pH 10.2, respectively. The thermal behaviours of these powders were analyzed using TG-DTA with a heating rate of 10 °C/min (Fig. 6). The DTA-curves in Fig. 6a show an endothermic region from 100 to 200 °C and an exothermic stage from 300 to 400 °C, which correspond to the dehydroxylation, the decomposition and combustion of the

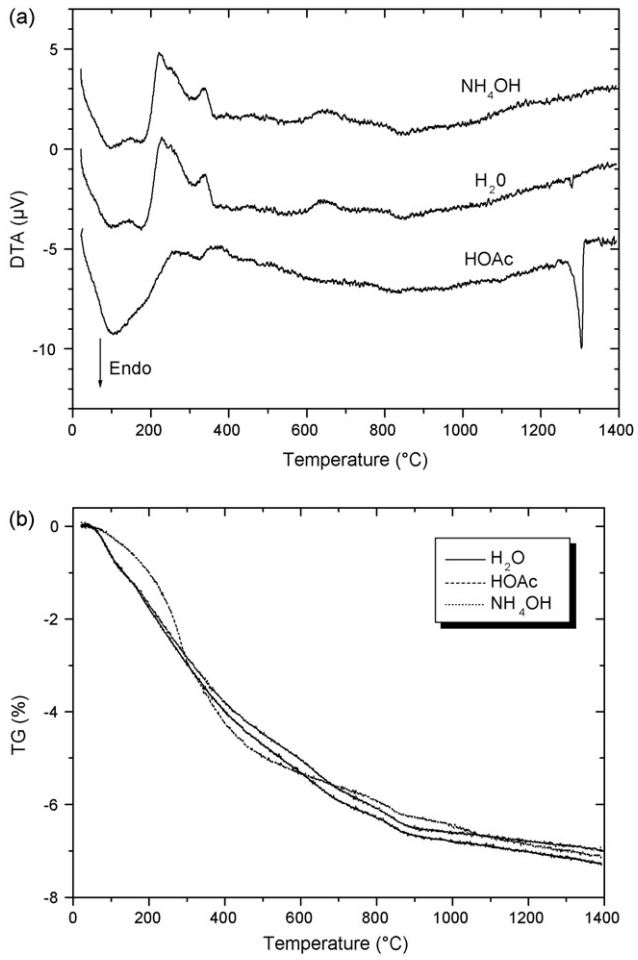

Fig. 6. (a) DTA and (b) TG diagrams of powders washed with different medium; Ba:Ti = 1.0.

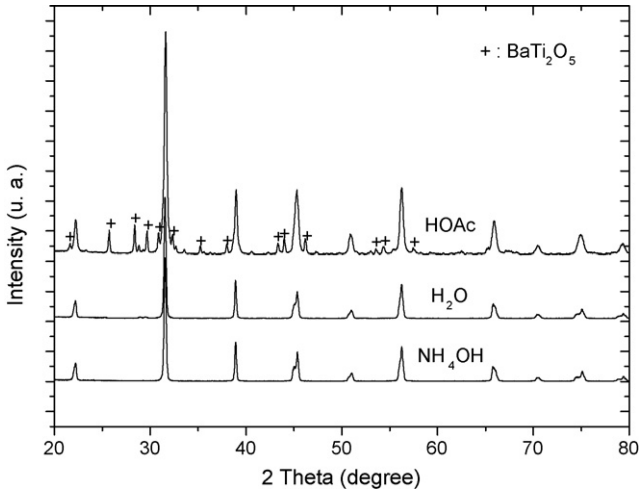

Fig. 7. XRD patterns of powders calcined at 1000 °C in dependence on the washing medium; Ba:Ti = 1.0.

remaining organic species in the powder, respectively. An obvious difference among the three samples lies at 1310 °C, where a small endothermic peak appears in the powder washed with water while no peak in the powder washed with ammonia and a sharp endothermic peak in the powder washed with the acetic acid (HOAc). The TG-curves (Fig. 6b) show a different weight-loss profile between the HOAc-sample and the other two samples at temperatures lower than 600 °C, which can be contributed to the adsorption of the HOAc acid on the particle surface. No obvious difference in weight-loss around 1310 °C can be found in the three curves, which suggests that the endothermic peak in the DTA-curve is due to the formation of a liquid phase. This can be confirmed from the phase diagram of $BaTiO_3$–TiO_2,[52] which shows the occurrence of the liquid phase at 1332 °C when the TiO_2 mol% in the powder is more than 50%.

To further clarify the formation of the liquid phase above 1310 °C in powders washed with water and acetic acid, the powders calcined at 1000 °C were analyzed with X-ray diffractometer (Fig. 7). It can be seen that an impure phase of $BaTi_2O_5$ exists in the powder washed with acetic acid. Its traces can be discerned (near $2\theta = 30°$) in the calcined powder washed with water. The calcined powder washed with ammonia consists nevertheless of a single-phase $BaTiO_3$.

It is well known that the surface of $BaTiO_3$ particle is rich of titanium dioxide at low pHs because of the barium dissolution. $BaTi_2O_5$ is thus formed through the reaction between $BaTiO_3$ and TiO_2 at temperatures above 1000 °C.

Washing the powder with the acetic acid has been used to remove $BaCO_3$ from $BaTiO_3$.[30,53] Acid cleaning the commercial powders could decrease the $BaCO_3$ content, and was therefore useful for limiting the abnormal grain growth.[54] However, it could not completely remove $BaCO_3$ from the powder. This means, the beneficial effect for sintering of acid cleaning was achieved through decreasing the impure content of the powder. The severe leaching of barium by acid washing in our case results in formation of the undesired $BaTi_2O_5$ phase at high temperatures. This impurity can promote the formation of a liquid phase, which will lead to the abnormal grain growth. Ammonia is effective to limit the leaching of barium from barium titanate powders and is therefore more suitable for cleaning of the synthesized powders.

3.6. Properties of the powder

The $BaTiO_3$ powder prepared with a Ba:Ti ratio of 1.0 and washed with the ammonia solution to pH 10.2 was observed under HRTEM. Its diffraction and contrast image (Fig. 8a) shows that the particles are agglomerated and aggregated with a size varying from 5 to 25 nm. Some particles show a clearly distinctive cubic habit. In the structure image, Fig. 8b two single particles can be seen. The right particle nevertheless results from the coalescence of two cubic formed particles which fused with mutually aligned lattice planes. The structure Fig. 8c shows the aggregation of two particles, in which their lattice orientation is not completely aligned.

The particle size distribution of the $BaTiO_3$ suspension (5 wt.%) after being ultrasonicated for 10 min is shown in Fig. 9. The value of d_{10}, d_{50} and d_{90} is 81, 137 and 239 nm, respectively. As the primary particle size lies in the range of 5–25 nm, the particles in the suspension are still agglomerated.

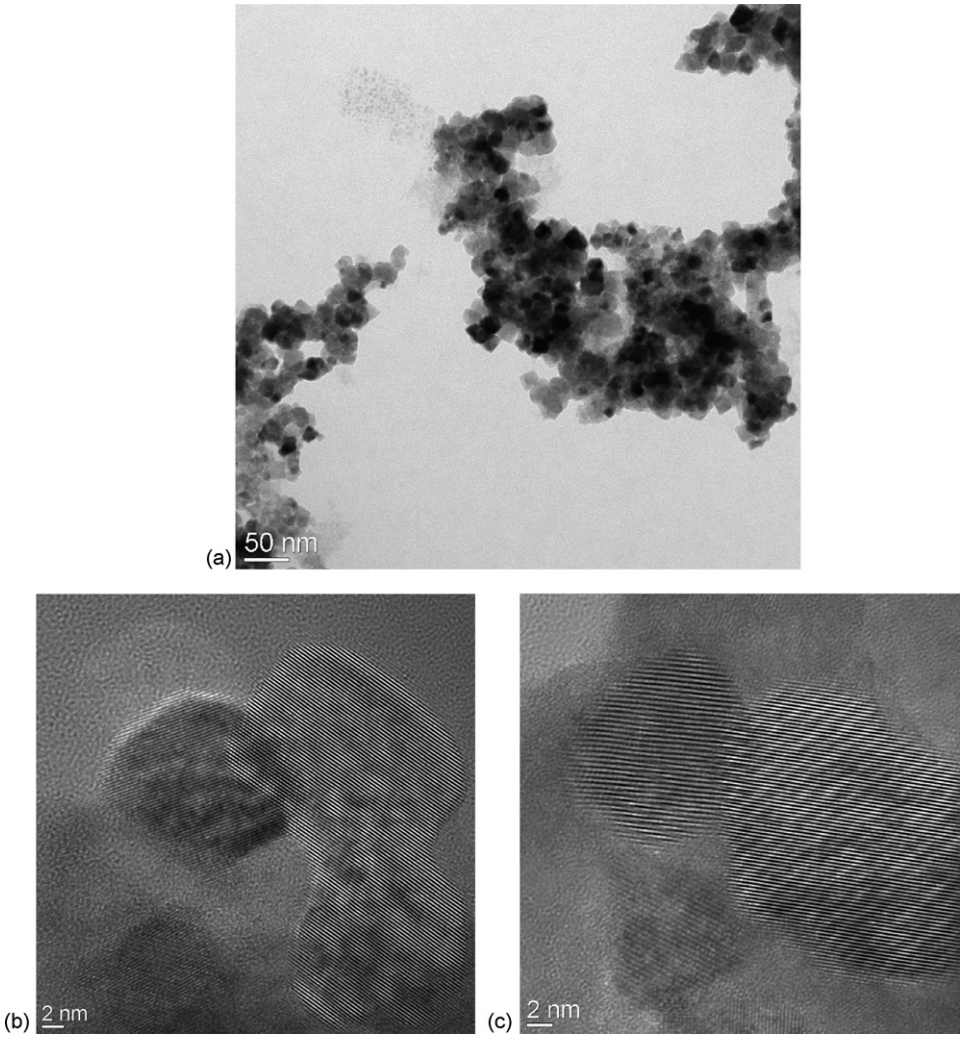

Fig. 8. HRTEM micrograph of $BaTiO_3$ powders with Ba:Ti = 1.0: (a) diffraction and contrast imaging and (b and c) structure imaging.

The BET specific surface area of the powder, which is affected by other parameters such as the addition speed of Tyzor TE to the $Ba(OH)_2$ solution and the synthesized amount varies in the range of 60–75 m^2/g. The powder density of 4.50–5.10 g/cm^3 is much less than its theoretic value (6.02 g/cm^3). This can be attributed to the increase in OH percentage on the surface of the $BaTiO_3$ nanoparticles with a crystallite size of 17–19 nm.

Fig. 10 indicates the dependence of the specific surface area (S) and the crystallite size (d) on the calcination temperature (T). The specific surface area decreases linearly with increasing temperature. Through fitting the curve, the relation between S and T can be described as:

$$S = 78.45 - 0.065T(\mathrm{m^2/g}) \quad (2)$$

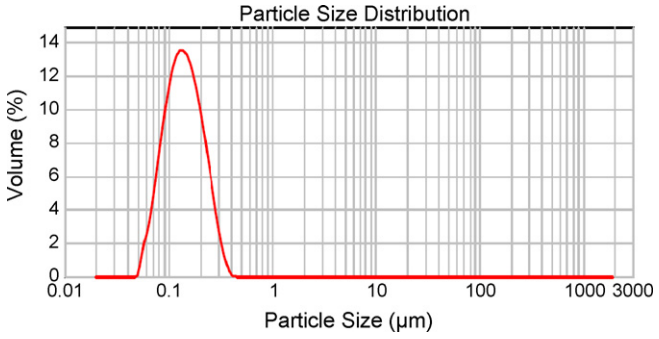

Fig. 9. Particle size distribution of the $BaTiO_3$ suspension (5 wt.%, Ba:Ti = 1.0).

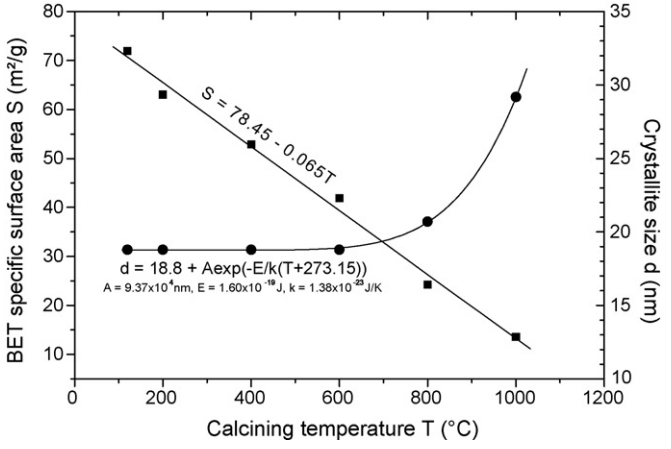

Fig. 10. Dependence of BET specific surface area and crystallite size on the calcining temperature for 1 h (Ba:Ti = 1.0).

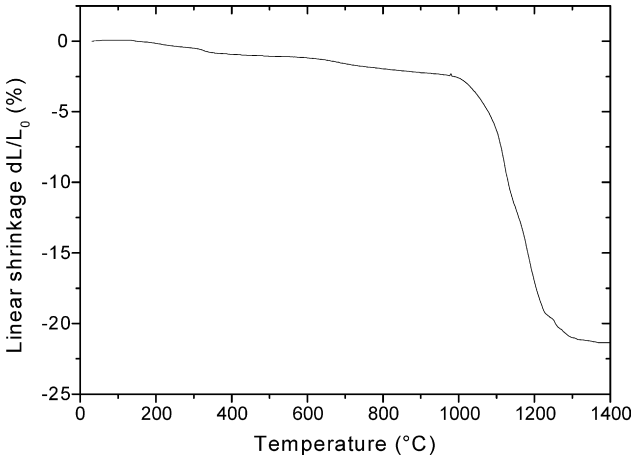

Fig. 11. Dilatometry curve of $BaTiO_3$ powder synthesized with the Ba:Ti ratio of 1.0 and the heating rate of 5 °C/min.

The crystallite grows slowly up to 600 °C and then increases substantially. The dependence of the crystallite size and temperature can be fitted with the equation:

$$d = 18.8 + A\,e^{[-(E/k(T+273.15))]} \quad (3)$$

where $A = 9.37 \times 10^4$ nm, $E = 1.60 \times 10^{-19}$ J and k is the Boltzmann's constant. We know in the powder the crystallite growth is dependant on the mass transport rate. The mass transport can be controlled either by surface diffusion along a surface when particles are separated from each other, or by volume diffusion, either along the grain boundaries or through the lattice dislocation if the particles contact with each other by formation of a neck. The diffusion coefficient (D) is dependent on the temperature (T). According to Arrhenius equation, there exists such a relation between them:

$$D = D_0\,e^{[-(E_D/k(T+273.15)]} \quad (4)$$

where E_D is the activation energy of diffusion and D_0 is a constant. The curve of the crystallite size in Fig. 9 reflects therefore a diffusion controlled growth process. E in Eq. (3) can be defined as the activation energy of the particle growth and is 1 eV. At low temperatures, the slow particle growth is realized through evaporation–condensation. From 600 °C, the grain-boundary diffusion is dominant after the neck formation between particles, and the particle growth becomes therefore fast.

3.7. Sintering of the powder

The shrinkage behaviour of the prepared $BaTiO_3$ powder (Ba:Ti = 1.0, washed with ammonia solution) was investigated by means of dilatometry. The cylindric sample with a diameter about 5 mm was formed at 400 MPa by isostatic pressing. The green density of the powder pellet is 2.88 g/cm^3 (47.8% of the theoretic density). The linear shrinkage curve of the sample is presented in Fig. 11. It can be seen that the sintering of the sample begins at about 1000 °C and ends around 1300 °C.

In the temperature range of 1000 and 1300 °C, the pellets with a dimension of Ø 10.7 mm × 2.7 mm pressed isostatically at 400 MPa were sintered for 0.5 h. A sintered sample with 94.7% of the theoretic density was obtained at 1250 °C. The ceramic cannot be further densified just by increasing the sintering temperature. The optimal sintering duration at 1250 °C was found to be 1–2 h. The ceramics with a high density of 5.77 g/cm^3 (95.8% of the theoretic density) is obtained at sintering at 1250 °C for 2 h.

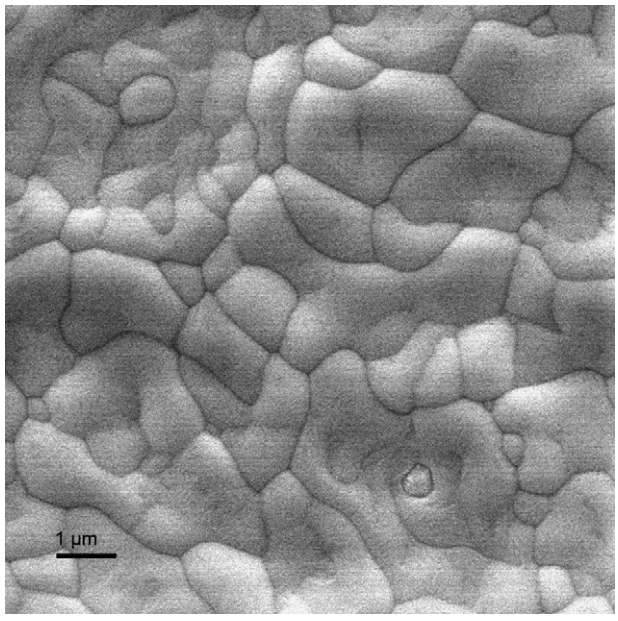

Fig. 12. SEM micrograph of $BaTiO_3$ ceramic sintered at 1250 °C for 1 h. The sample was thermally etched at 1150 °C for 30 min.

The micrograph of the $BaTiO_3$ sample sintered at 1250 °C for 1 h is shown in Fig. 12. The grain size varied from 0.3 to 2 µm indicating an abnormal grain growth. Redispersing the nanoparticles to their primary size could be a possible way to limit the abnormal grain growth of particles at high temperatures.

The temperature dependence of the dielectric properties of the ceramic sintered at 1250 °C for 1 h at several frequencies are shown in Fig. 13. The values of the dielectric constants at room temperature vary between 3400 and 4200 depending

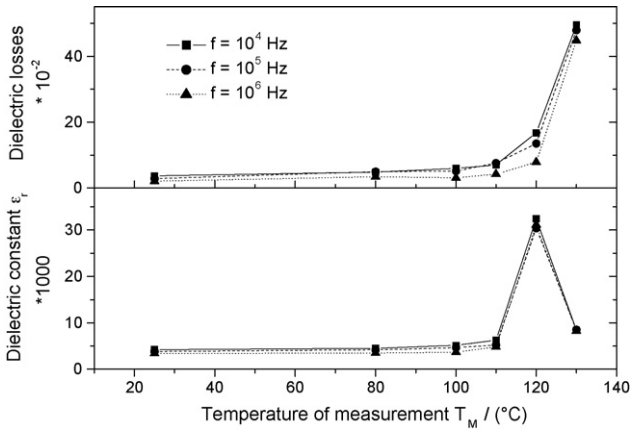

Fig. 13. Dielectric constants and dielectric losses of $BaTiO_3$ ceramics sintered at 1250 °C for 1 h depending on the temperature of measurement for measurements at 10, 100 kHz and 1 MHz.

on frequency. This is comparable to the results described in literature.[3,55–57] Dielectric constants up to nearly 33,000 were observed near the Curie temperature of 120 °C. However, the dielectric loss of the ceramics with values of 0.021–0.037 at room temperature is high.

4. Conclusions

$BaTiO_3$ particles with a size of 5–25 nm and a large specific surface area of 60–75 m^2/g have been prepared by coprecipitating of a titanium ester and a $Ba(OH)_2$ solution under refluxing conditions. The concentration of $Ba(OH)_2$ affects the particle size and the surface area. A higher $Ba(OH)_2$ concentration will lead to an increase in the agglomeration and aggregation degree of the particles. The addition of isopropanol at the starting solution for replacing water has been found to be effective for increasing the surface area and lowering the particle size. Its optimal concentration lies at the volume rate of water to isopropanol = 1.0. When excess barium ions or amorphous titanium oxide exist in the as-prepared powder, they could react with $BaTiO_3$ at high temperatures, form undesired phases and affect the tetragonality of $BaTiO_3$. The leaching of the barium ions during processing at low pHs has also been found in the prepared nanoscaled powders. It leads to the formation of $BaTi_2O_5$ around 1000 °C and promotes the formation of a liquid phase around 1310 °C, which will be negative to the powder sintering. The barium ions can nevertheless be fixed in the powder by washing with ammonia solution to pH 10.2. The surface area of the powder decreases linearly with increasing in calcining temperature. The sintering of the samples begins around 1000 °C and a dense $BaTiO_3$ ceramic (95.8% of the theoretic density) has been obtained by sintering at 1250 °C for 2 h. The ceramic with a grain size of 0.3–2 μm exhibits a high dielectric constant but also a high dielectric loss.

Acknowledgement

The authors would like to thank Dr. U. Werner for the high resolution electron microscopy and his helpful discussion.

References

1. Unruh, H. G., *Ferroelectrics in Ullmann's Encyclopaedia of Industrial Chemistry* (*electronic ed.*). Wiley-VCH Verlag, 2002.
2. Gablenz, S, *Sprühtrocknung und Sprühhydrolyse—neue Methoden zur Herstellung von Metalloxiden und zur Modifizierung von $BaTiO_3$*. Thesis of Martin-Luther-University Halle-Wittenberg, 2002.
3. Dutta, P. K., Asiaie, R., Akbar, S. A. and Zhu, W., Hydrothermal synthesis and dielectric properties of tetragonal $BaTiO_3$. *Chem. Mater.*, 1994, **6**, 1542–1548.
4. Kumar, K., Ceramic capacitors: an overview. *Electron. Inf. Plann.*, 1998, **25**(11), 559–582.
5. Rae, A., Chu, M. and Ganinie V, In *Barium Titanate—Past, Present and Future in Ceramic Transactions, vol. 100: Dielectric Ceramic Materials*, ed. K. M. Nair and A. S. Bhalla. American Ceramic Society, Westerville, OH, 1999, pp. 1–12.
6. Cott, J., Status report on ferroelectric memory materials. *Integr. Ferroelectr.*, 1998, **20**(1–4), 15–23.
7. Buchal, C. and Siegert, M., Ferroelectric thin films for optical applications. *Integr. Ferroelectr.*, 2001, **35**(1–4), 1731–1740.
8. Alles, A. B. and Burdick, V. L., Grain-boundary oxidation in PTCR barium–titanate thermistors. *J. Am. Ceram. Soc.*, 1993, **76**(2), 401–408.
9. Zhou, Z., Zhao, G., Wei, M. and Zhang, Z., Temperature–humidity-gas multifuntional senstive ceramics. *Sens. Actuators*, 1989, **19**, 71–81.
10. Mori, M., Kineri, T., Kadono, K., Sakaguchi, T., Miya, M., Wakabayashi, H. *et al.*, Effect of the atomic ratio of Ba to Ti on optical-properties of gold-dispersed $BaTiO_3$ thin-films. *J. Am. Ceram. Soc.*, 1995, **78**(9), 2391–2394.
11. Venigalla, S., Advanced materials and powders digest-barium titanate. *Am. Ceram. Soc. Bull.*, 2001, **80**, 63–64.
12. Costantino, S. A., Hard, R. A., Venigalla, S., Dispersile, metal oxide-coated, barium titanate materials. US 6268054, 2001.
13. Templeton, L. K. and Pask, J. A., Formation of $BaTiO_3$ from $BaCO_3$ and TiO_2 in air and in CO_2. *J. Am. Ceram. Soc.*, 1959, **42**(5), 212–216.
14. Beauger, A., Mutin, J. C. and Niepce, J. C., Synthesis reaction of metatitanate $BaTiO_3$-part 2: study of solid–solid interfaces. *J. Mater. Sci.*, 1983, **18**, 3543–3550.
15. Pfaff, G., Sol–gel synthesis of barium titanate powders of various compositions. *J. Mater. Chem.*, 1992, **2**(6), 591–594.
16. Moreno, J., Dominguez, J. M., Montoya, A., Vicente, L. and Viveros, T., Synthesis and characterization of $MTiO_3$ (M = Mg, Ca, Sr, Ca). *J. Mater. Chem.*, 1995, **5**(3), 509–512.
17. Kuo, W. and Ling, Y., Effects of mono-substituting chelating agents on $BaTiO_3$ prepared by the sol–gel process. *J. Mater. Sci.*, 1994, **29**, 5625–5630.
18. Pechini, M. P. Barium titanium citrate, barium titanate and processes for producing same. Patent US3231328, 1966.
19. Stockenhuber, M., Mayer, H. and Lercher, J. A., Preparation of barium titanates from oxalates. *J. Am. Ceram. Soc.*, 1993, **76**(5), 1185–1190.
20. Wada, S., Narahara, M., Hoshina, T., Kakemono, H. and Tsurumi, T., Preparation of nm-sized $BaTiO_3$ particles using a new 2-step thermal decomposition of barium titanyl oxalate. *J. Mater. Sci.*, 2003, **38**, 2655–2660.
21. Dutta, P. K. and Gregg, J. R., Hydrothermal synthesis of tetraganol barium titanate. *Chem. Mater.*, 1992, **4**, 843–846.
22. Clark, I. J., Takeuchi, T., Ohtor, N. and Sinclair, D., Hydrothermal synthesis and characterisation of $BaTiO_3$ fine powders: precursors, polymorphism and properties. *J. Mater. Chem.*, 1999, **9**, 83–91.
23. Moon, J., Kerchner, J. A., Krarup, H. and Adair, J. H., Hydrothermal synthesis of ferroelectric perovskites from chemically modified titanium isoproxide and acetate salts. *J. Mater. Res.*, 1999, **14**(2), 425–435.
24. Flaschen, S. S., An aqueous synthesis of barium titanate. *J. Am. Chem. Soc.*, 1955, **77**(12), 6194.
25. Kiss, K., Magder, J., Vukasovich, M. S. and Lockhart, R. J., Ferroelectrics of ultrafine particle size: I. Synthesis of titanate powders of ultrafine particle size. *J. Am. Ceram. Soc.*, 1966, **49**(6), 291–295.
26. Kumar, V., Solution-precipitation of fine powders of barium titanate and strontium titanate. *J. Am. Ceram. Soc.*, 1999, **82**(10), 2580–2584.
27. Moon, J., Suvaci, E., Li, T., Costantino, S. A. and Adair, J. H., Phase development of barium titanate from chemically modified-amorphous titanium (hydrous) oxide precursor. *J. Eur. Ceram. Soc.*, 2002, **22**(6), 809–815.
28. Hung, K., Yang, W. and Huang, C., Preparation of nanometer-size barium titanate powders by a sol-precipitated process with surfactants. *J. Eur. Ceram. Soc.*, 2003, **23**, 1901–1910.
29. Kamiya, H., Gomi, K., Iida, Y., Tanaka, K., Yoshiyasu, T. and Kakiuchi, T., Preparation of highly dispersed ultrafine barium titanate powder by using microbial-derived surfactant. *J. Am. Ceram. Soc.*, 2003, **86**(12), 2011–2018.
30. Nanni, P., Leoni, M. and Buscaglia, V., Low-temperature aqueous preparation of barium metatitanate powders. *J. Eur. Ceram. Soc.*, 1994, **14**, 85–90.
31. Viviani, M., Buscaglia, M. T., Testino, A., Buscaglia, V., Bowen, P. and Nanni, P., The influence of concentration on the formation of $BaTiO_3$ by direct reaction of $TiCl_4$ with $Ba(OH)_2$ in aqueous solution. *J. Eur. Ceram. Soc.*, 2003, **23**, 1383–1390.
32. Testino, A., Buscaglia, M. T., Viviani, M., Buscaglia, V. and Nanni, P., Synthesis of $BaTiO_3$ particles with tailored size by precipition from aqueous solutions. *J. Am. Ceram. Soc.*, 2004, **87**(1), 79–83.
33. Testino, A., Buscaglia, M. T., Buscaglia, V., Viviani, M., Bottino, C. and Nanni, P., Kinetics and mechanism of aqueous chemical synthesis of $BaTiO_3$ particles. *Chem. Mater.*, 2004, **16**, 1536–1543.
34. Testino, A., Buscaglia, M. T., Buscaglia, V., Viviani, M., Bottino, C. and Nanni, P., Kinetic modeling of aqueous and hydrothermal syn-

thesis of barium titanate ($BaTiO_3$). *Chem. Mater.*, 2005, **17**, 5336–5346.
35. Wang, X., Lee, B. I., Hu, M. Z., Payzant, E. A. and Blom, D. A., Synthesis of nanocrystalline $BaTiO_3$ by solvent refluxing method. *J. Mater. Sci. Lett.*, 2003, **22**(7), 557–559.
36. Lee, B. I., Wang, M., Yoon, D. and Hu, M. Z., Aqueous processing of barium titanate powders. *J. Ceram. Process Res.*, 2003, **4**(1), 17–24.
37. Her, Y., Matijevic, E. and Chon, M. C., Preparation of well-defined colloidal barium titanate crystals by the controlled double-jet precipitation. *J. Mater. Res.*, 1995, **10**(12), 3106–3114.
38. Uchino, K., Sadanaga, E. and Hiose, T., Dependance of the crystal structure on particle size in barium Titanate. *J. Am. Ceram. Soc.*, 1989, **72**(8), 1558–1658.
39. Zhong, W., Wang, Y., Zhang, P. and Qu, B., Phenomenological study of the size on phase transitions in ferroelectric particles. *Phys. Rev. B*, 1994, **50**(2), 698–703.
40. Frey, M. H. and Payne, D. A., Grain-size effect on structure and phase transformations for barium titanate. *Phys. Rev. B*, 1996, **54**(5), 3158–3168.
41. McCauley, D., Newnham, R. E. and Randall, C. A., Intrinsic size effects in a barium titanate glass-ceramic. *J. Am. Ceram. Soc.*, 1989, **81**(4), 979–987.
42. Tsunekawa, S., Ito, S., Mori, T., Ishikawa, K., Li, Z. and Kawazoe, Y., Critical size and anomalous lattice expansion in nanocrystalline $BaTiO_3$ particle. *Phys. Rev. B*, 2000, **61**(5), 3065–3070.
43. Böttcher, R., Klimm, C., Michel, D., Semmelhack, H.-C., Vökel, G., Gläsel, H.-J. *et al.*, Size effect in Mn^{2+}-doped $BaTiO_3$ nanopowders observed by electron paramagnetic resonance. *Phys. Rev. B*, 2000, **62**(3), 2085–2095.
44. Saad, M. M., Baxter, P., Bowman, R. M., Gregg, J. M. and Morrison, F. D., Intrinsic dielectric response in ferroelectric nano-capacitors. *J. Phys. Condens. Matter*, 2004, **16**, L451–L456.
45. Buscaglia, V., Buscaglia, M. T., Viviani, M., Mitoseriu, L., Trafiletti, Piaggio, P. *et al.*, Grain size and grain boundary-related effects on the properties of nanocrystalline barium titanate ceramics. *J. Eur. Ceram. Soc.*, 2006, **26**, 2889–2898.
46. Li, X. and Shih, W., Size effects in barium titanate particles and clusters. *J. Am. Ceram. Soc.*, 1997, **80**(11), 2844–2852.
47. Kobayashi, Y., Nishikata, A., Tanase, T. and Konno, M., Size effect on crystal structures of barium titanate nanoparticles prepared by a sol-gel method. *J. Sol–Gel Sci. Techn.*, 2004, **29**, 9–55.
48. Schrerrer, P. Gött. Nachrichten, Conference on July 26, 1918, 99–100.
49. Lencka, M. M. and Rieman, R. E., Thermodynamic modelling of hydrothermal synthesis of ceramic powders. *Chem. Mater.*, 1993, **5**, 61–70.
50. Anderson, D. A., Adair, J. H., Biggers, J. V. and Shrout, T. R., In *Surface Chemistry Effects on Ceramic Processing of $BaTiO_3$ powder. Ceramic Transactions, vol. 1, Ceramic Powder Science II*, ed. G. L. Messing, E. K. Fuller Jr. and H. Hausner. American Ceramic Society, Westerville, OH, 1988, pp. 485–492.
51. Neubrand, A., Lindner, R. and Hoffmann, P., Room-temperature solubility behaviour of barium titanate in aqueous media. *J. Am. Ceram. Soc.*, 2000, **83**, 860–864.
52. Ritter, J. J., Roth, R. S. and Blendell, J. E., Alkoxide precursor synthesis and characterization of phases in the barium–titanium oxide system. *J. Am. Ceram. Soc.*, 1986, **69**(2), 155–162.
53. Hérard, C., Faivre, A. and Lemaitre, J., Surface decontamination treatments of undoped $BaTiO_3$-part I: powder and green body properties. *J. Eur. Ceram. Soc.*, 1995, **15**, 135–143.
54. Hérard, C., Faivre, A. and Lemaitre, J., Surface decontanination treatments of undoped $BaTiO_3$-Part II: influence on sintering. *J. Eur. Ceram. Soc.*, 1995, **15**, 145–153.
55. Chen, R. Z., Wang, X., Gui, Z. L. and Li, L. T., Effect of silver addition on the dielectric properties of barium titanate based X7R ceramics. *J. Am. Ceram. Soc.*, 2003, **86**(6), 1022–1024.
56. McCormick, M. A. and Slamovich, E. B., Microstructural development and dielectric properties of hydrothermal $BaTiO_3$ thin films. *J. Eur. Ceram. Soc.*, 2003, **23**, 2143–2152.
57. Miot, C., Proust, C. and Husson, E., Dense ceramics of $BaTiO_3$ produced from powders prepared by a chemical process. *J. Eur. Ceram. Soc.*, 1995, **15**, 1163–1170.